Interferometric data analysis based on Markov nonlinear filtering methodology

Igor P. Gurov and Denis V. Sheynihovich

Saint Petersburg Institute of Fine Mechanics and Optics (Technical University), 14 Sablinskaya Street, Saint Petersburg 197101, Russia

Received March 15, 1999; revised manuscript received July 15, 1999; accepted August 2, 1999

For data processing in conventional phase shifting interferometry, Fourier transform, and least-squares-fitting techniques, a whole interferometric data series is required. We propose a new interferometric data processing methodology based on a recurrent nonlinear procedure. The signal value is predicted from the previous step to the next step, and the prediction error is used for nonlinear correction of an *a priori* estimate of the parameters phase, visibility, or frequency of interference fringes. Such a recurrent procedure is correct on the condition that the noise component be a Markov stochastic process realization. The accuracy and stability of the recurrent Markov nonlinear filtering algorithm were verified by computer simulations. It was discovered that the main advantages of the proposed methodology are dynamic data processing, phase error minimization, and high noise immunity against the influence of non-Gaussian noise correlated with the signal and the automatic solution of the phase unwrapping problem. © 2000 Optical Society of America [S0740-3232(99)01012-1]

OCIS codes: 050.5080, 070.6020, 030.4280, 100.5070.

1. INTRODUCTION

The phase restoration of interference fringes is widely used in wave-front analysis,[1–3] dimensional metrology and testing,[2,4–7] and surface characterization.[3,8] Interferometric data are often distorted by the influence of illumination and background nonuniformity, speckle noise, and phase fluctuations. Interference patterns can be represented by the interferometric signal model

$$S(x, y, \mathbf{\Theta}) = S_b(x, y) + S_e(x, y)\cos\Phi(x, y, \mathbf{\Theta}_\phi) + N_a(x, y), \tag{1}$$

where S_b is the background component, S_e is the envelope function, $\Phi = E + \phi(x, y)$, E is the fractional part of the phase cycle 2π at the point $(x = 0, y = 0)$, $\phi(x, y)$ is the phase deviation with its own vector of parameters $\mathbf{\Theta}_\phi$, N_a is the additive noise, and $\mathbf{\Theta} = (S_b, S_e, \Phi, \mathbf{\Theta}_\phi^{\mathbf{T}})^{\mathbf{T}}$ is the vector of parameters. The parameter $\mathbf{\Theta}_\phi$ defines the form of the phase deviation function $\phi(x, y)$ in the parametric form. For example, in the case of the linear function $\phi(x, y) = U_x x + U_y y$, the vector $\mathbf{\Theta}_\phi = (U_x, U_y)^{\mathbf{T}}$, where U_x, U_y are the circular frequencies of interference fringes along the x and y axes, respectively. In general, the parameters U_x, U_y may depend on x and y, respectively.

The essence of interferometric data analysis is the solution of the nonlinear inverse problem of the phase function $\Phi(x, y, \mathbf{\Theta}_\phi)$ restoration by processing of the signal $S(x, y, \mathbf{\Theta})$ under the condition that $\mathbf{\Theta}$ contain components with *a priori* unknown values.

Conventional methods used to solve this problem may be classified by the concept of multidimensional (multichannel) interferometric signal analysis[9] that represents the interferometric data in the form

$$S_k = S(x_k, y_k, \mathbf{\Theta}_k),$$

where k is the pair (p, q) of numbers, $p, q = 0, 1,...$; that is, $x_k = p\Delta x$, $y_k = \Delta y$, where Δx, Δy are the two-dimensional-discretization steps of the interference fringes. The multidimensional interferometric signal

$$\mathbf{S}_k{}^d = (S_k{}^d, S_{k-1}{}^d, \ldots, S_{k-N}{}^d)^{\mathbf{T}} \tag{2}$$

represents $(N + 1)$ samples of a single interference pattern, and the multichannel interferometric signal

$$\mathbf{S}_m^c = (S_{0m}^c, S_{1m}^c, \ldots, S_{km}^c, \ldots, S_{Km}^c)^{\mathbf{T}} \tag{3}$$

contains the signal values detected simultaneously in $(K + 1)$ points of $(M + 1)$ interference patterns with temporal separation between them.

For processing the signal [Eq. (2)], the Fourier transform method[4,6,7] is often used, which is mathematically equivalent to the convolution method.[10,11] To reduce the systematic error of spectral analysis and restore the analytical signal argument[10] with high accuracy, this method requires that the interference pattern contain a large, preferably integer number of fringes. The method is performed by increasing the tilt between the reference and the test wave fronts.[4,7] The phase retrieval accuracy depends on the extent of the interference pattern and the form of the edge of the interference pattern area.[6,7]

The phase shifting interferometry (PSI) technique proposed by Bruning *et al.*[1] is more accurate. The phase stepping process may be represented by a vector signal [Eq. (3)], where m is the phase step number, $m = 0, 1,..., M$, $M \geqslant 2$.

The PSI method is widely used in optical metrology and testing[2,12] and in x-ray interferometry.[13] Simple data processing algorithms are usually realized, but it is difficult to optimize such methodology for the increasing accuracy and noise immunity of the totality of the data because of the nonlinear nature of the data transform. Some effective techniques and data correction algorithms

for error reduction were proposed in recent years.[14–19] The basic approach was usually selected as a least-squares fitting of the interferometric data series and phase estimation under the condition that the least-squares-fitting error be minimized.[13,15,18]

It is well known that such an approach gives effective and unbiased estimates when the data noise is Gaussian, additive, and uncorrelated.[20] The real interferometric data series are distorted by phase fluctuations,[21] phase shifting nonlinearity,[18,19,22] and signal-dependent noise.[13] In these cases the least-squares-fitting approach is generally not optimal and can give incorrect phase estimation results. In addition, an important problem is the noise-immune phase unwrapping[8] at intervals greater than 2π.

The phase and intensity of interference fringes depend on each other nonlinearly. Therefore it is reasonable to minimize the phase error directly by nonlinear filtering of an interferometric data series [Eq. (2) or Eq. (3)]. We propose a nonlinear filtering method based on the theory of the Markov stochastic process for accurate phase estimation of a distorted interferometric data series. The Markov nonlinear filtering (MNLF) method is realized as a recurrence procedure and can be used for dynamic signal processing. The signal value is predicted from the previous step to the next step, and the prediction error is used for nonlinear step-by-step correction of an *a priori* estimate of the parameters phase, visibility, or frequency of interference fringes. It will be shown that the MNLF method ensures high noise immunity and accuracy against the influence of background nonuniformity, phase fluctuations, and correlated Gaussian noise.

2. THEORY

The Markov theory of optimal nonlinear filtering[23] was developed for a wide class of data processing problems for which an optimal filtering problem could not be solved earlier. The advantage of the recurrence MNLF methodology is that it is free from essential restrictions that are inherent to other methods, such as Kalman–Bucy linear filtering.[24] The requirement that the stochastic component has to be the Markov process realization is not very strict, since a real stochastic process can be approximated by the Markov process with any degree of accuracy.[23]

Let us consider a component of a multichannel interferometric signal [Eq. (3)] in the form (upper indices are omitted to simplify the notation)

$$S_k = S_{b_k} + S_{e_k}\cos(\Phi_k + N_{ph_k}) + N_{a_k}, \tag{4}$$

where $\Phi_k = \Sigma_{k'=0}^{k} U_{k'}\Delta x + E$; $U_{k'}$ is the circular frequency; E is the initial phase at point $k = 0$; x_k is the argument; $S_{b_k} = S_b(x_k)$ are *a priori* unknown background component samples; $S_{e_k} = S_e(x_k)$ are *a priori* unknown envelope function samples of interference fringes; $N_{a_k} = N_a(x_k)$ are the additive white-noise sample series with characteristics $\mathrm{M}[N_{a_k}] = 0$, $\mathrm{M}[N_k N_{k+n}] = \sigma_a{}^2\delta(n)$; σ_a is the noise variance; M[.] is the average over the ensemble of frames; $\delta(n)$ is the delta function; and N_{ph_k} is the phase fluctuation represented by correlated noise. Usually correlated noise can be described by the first-order stochastic differential equation

$$\frac{\mathrm{d}N_{ph}(x)}{\mathrm{d}x} = -\alpha N_{ph}(x) + \alpha w(x), \tag{5}$$

where $w(x)$ is white-Gaussian-noise realization (the "forming" noise), $\mathrm{M}[w(x)] = 0$, $\mathrm{M}[w(x)w(x+\chi)] = N_0\delta(\chi)$, and α is a constant. It is well known[23] that the spectral density of the process described by Eq. (5) is defined in the form

$$G_{N_{ph}}(u) = \frac{\alpha^2 N_0}{2(\alpha^2 + u^2)}. \tag{6}$$

The normalized value spectral density Eq. (6) is illustrated in Fig. 1. The spectrum width on level 0.5 is defined by the value of α. The lower α is, the faster the spectral density of process $N_{ph}(x)$ decreases; i.e., the more the noise is correlated.

The proof that phase fluctuations described by Eq. (5) correspond to the Markov process is given by the Doob theorem.[25] Discrete approximation of Eq. (5) has the form

$$N_{ph_k} = N_{ph_{k-1}}(1-\alpha)\Delta x_k + \alpha w_k,$$

where $\Delta x_k = x_k - x_{k-1}$, w_k is the Gaussian stochastic series.

Interferometric signal parameters in Eq. (4) may be taken into account as vector $\boldsymbol{\Theta} = (S_b, S_e, U, E)^{\mathbf{T}}$ components and can be estimated by processing signal samples $S(x_k)$.

For simplicity, let the signal parameters be $S_{b_k} = A = \text{const}$ and $S_{e_k} = AV\exp(-C_k{}^2)$, where $C_k = (x_k - x_0)B_k$ and V is the visibility at the point $x_k = x_0$, x_0 is the position of the envelope maximum, and B_k is the width envelope parameter. The model of the form of Eq. (4) can be rewritten in the form $S_k = S_k(x_k, \bar{\boldsymbol{\Theta}}_k)$, where $\bar{\boldsymbol{\Theta}} = [\Phi, U, C, B, V,]^{\mathbf{T}}$. The interferometric data series can be presented in the form

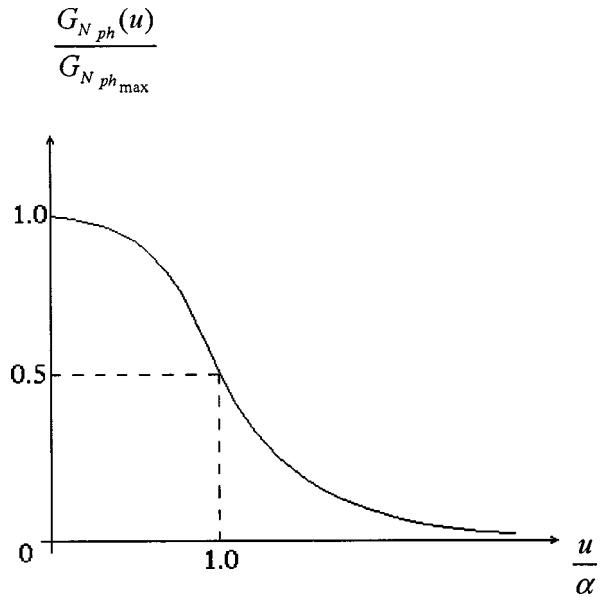

Fig. 1. Spectral density of the stochastic process described by Eq. (6).

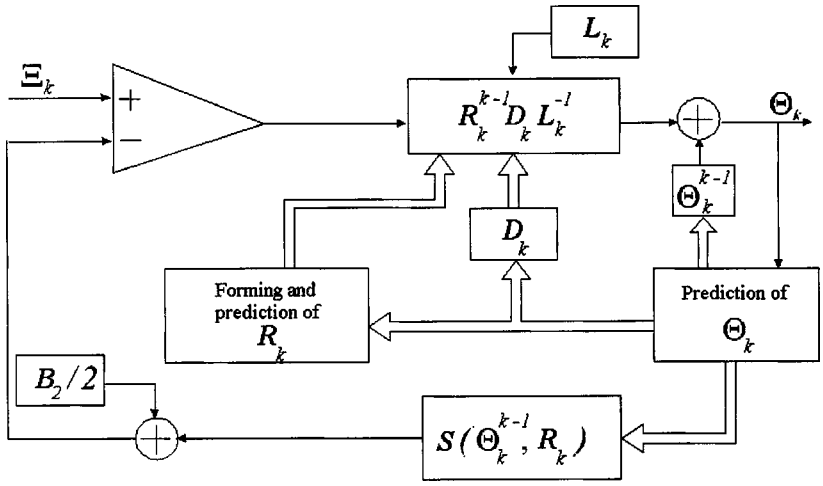

Fig. 2. Structure of the system for optimal nonlinear processing of phase shifting interferometric data.

$$\Xi_k = A[1 + V\exp(-C_k{}^2)\cos(\Phi_k + N_{ph_k})] + N_{a_k}. \quad (7)$$

The problem is to estimate the vector $\bar{\Theta}$ at the point x_k as the result of processing the data measured by point x_{k-1} in the Eq. (7) series.

To solve the problem, let us include the phase fluctuation component N_{ph} in the vector of parameters Θ, namely,

$$\Theta = [\Phi,\ U,\ C,\ B,\ V,\ N_{ph}]^{\mathbf{T}} \quad (8)$$

and consider the data as the function $S_k = S_k(x_k, \Theta_k)$. So the analyzed model is

$$\Xi_k = S_k(x_k, \Theta_k) + N_{a_k}.$$

Let us first assume that the components of the vector Θ change continuously. Using this assumption and the simplifications described above, we can consider the problem as the solution of the vector stochastic differential equation

$$\frac{d\Theta}{dx} = \mathbf{F}(x, \Theta) + \mathbf{G}(x, \Theta)\mathbf{N}(x),\ M[\mathbf{N}(x)] = 0,$$

$$M[\mathbf{N}(x)\mathbf{N}(x + \chi)] = N_0{}^2\delta(\chi), \quad (9)$$

where

$$\mathbf{F}(x, \Theta) = [U, 0, B, 0, 0, -\alpha N_{ph}],$$

$$\mathbf{G}(x, \Theta) = \mathbf{G} \text{ is a } (6 \times 6) \text{ matrix},$$

$$\mathbf{G}_{ij} = 0, \quad i, j = 1, \ldots, 5, \quad G_{66} = \alpha. \quad (10)$$

As mentioned above, the Doob theorem confirms that the process described with Eq. (9) is the Markov stochastic diffusion process.

Using this representation of the vector of parameters and taking into account all simplifications described above, we can present an estimation algorithm (see Appendix A) in the following form:

$$\Theta_k = \Theta_k^{k-1} + \mathbf{R}_k^{k-1}\mathbf{D}_k[\Xi_k - S(x_k, \Theta_k^{k-1}) - B_2/2]L_k^{-1}, \quad (11a)$$

$$\mathbf{R}_k = \mathbf{R}_k^{k-1}(\mathbf{I} - \mathbf{D}_k\mathbf{D}_k{}^{\mathbf{T}}\mathbf{R}_k^{k-1}L_k^{-1}), \quad (11b)$$

where $\mathbf{R}$ is the covariance matrix of parameters, $\mathbf{D}$ is the sensitivity vector that includes the partial derivatives of the signal model [Eq. (4)] with respect to the components of the vector of parameters, Ξ_k is the series of measured scalar values of the interferometric signal samples [Eq. (7)], $S(x_k, \Theta_k^{k-1})$ is the series of predicted values of the signal samples, $B_2/2$ is the correction coefficient of the Gaussian approximation of the second-order of the probability density function[23] (see Appendix A), L_k^{-1} is the dynamic filter amplification factor $L_k = \sigma_a{}^2 + \mathbf{D}_k{}^{\mathbf{T}}\mathbf{R}_k^{k-1}\mathbf{D}_k + B_3/2$, B_3 is defined by derivatives of the signal with respect to the components of the vector of parameters of the second order (see Appendix A), and $\mathbf{I}$ is the unit matrix. The upper index $(k-1)$ denotes the prediction from the previous step. The method for obtaining formulas (11) is outlined in Appendix A.

Now we can present the structure of the processing system synthesized with the concept of a recurrence MNLF methodology.[26] A schematic diagram of the system is given in Fig. 2. Its structure is clearly defined by Eqs. (11).

3. COMPUTER SIMULATIONS

To compare the MNLF algorithm with the well-known conventional PSI method, we assume that $S_{e_k} = S_e$, $S_{b_k} = S_b$, S_e, S_b are *a priori* unknown constants and take the vector of parameters $\Theta = [\Phi, U, V, N_{ph}]^{\mathbf{T}}$, where $U = 2\pi/P$, P is the unknown fixed number of samples on the 2π phase cycle, and $V = S_e/S_b$. Then the vector of derivatives in Eqs. (11) takes the form

$$\mathbf{D}_k = \left\{\left(\frac{\partial}{\partial\Theta_k^{k-1}}\right)^{\mathbf{T}}\right\} S(x_k, \Theta_k^{k-1})$$

$$= \begin{bmatrix} -AV_k^{k-1}\sin[\Phi_k^{k-1} + (N_{ph})_k^{k-1}] \\ 0 \\ 0 \\ -AV_k^{k-1}\sin[\Phi_k^{k-1} + (N_{ph})_k^{k-1}] \end{bmatrix}. \quad (12)$$

The coefficients B_2 and B_3 for this case are calculated in Appendix A under the assumptions described above.

The accuracy of optimal phase estimation by the MNLF method was verified[27] by processing the computer-simulated data series defined by Eqs. (11). We assumed

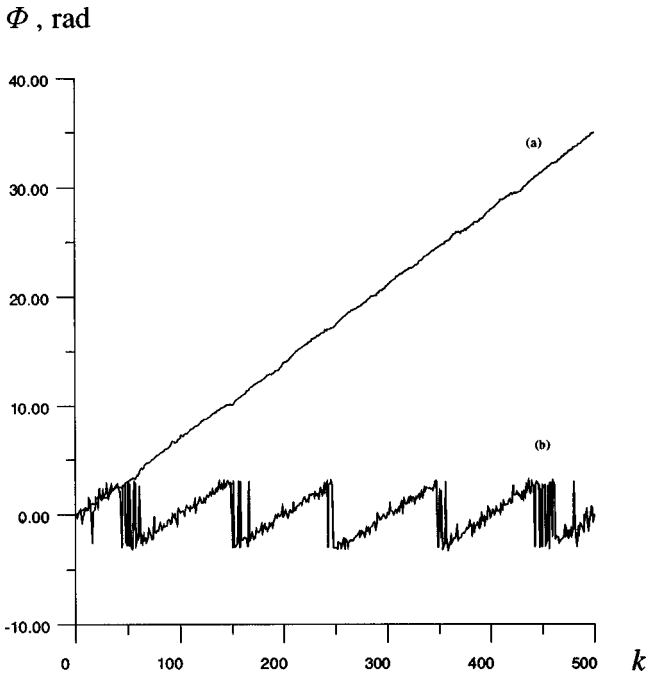

Fig. 3. Phase recovered by the MNLF algorithm [curve (a)], and the PSI method [curve (b)].

that speckle noise affects the data series both as additive noise N_a and phase fluctuation N_{ph}. It was discovered that under conditions of speckle noise the MNLF method provides stable phase recovery and the problem of phase unwrapping is solved automatically, because at each step the value of the unwrapped phase function Φ [Eq. (4)] is calculated by the recurrent procedure considered above. To illustrate this property, we compared results of the MNLF algorithm and the conventional PSI method. The results are shown in Fig. 3.

The phase data restored by the MNLF algorithm are presented by curve (a). The data series S_k processed by a four-step PSI method with phase shifts $\pi/2$ is illustrated by curve (b). In this graph one can clearly see the 2π unstableness effect that is inherent in the PSI method. This disadvantage is eliminated by the MNLF algorithm.

The results of accurate verification of phase recovery under the influence of phase fluctuation and additive noise are illustrated in Figs. 4 and 5. In Fig. 4 an example of phase estimation for selected phase values of $\Phi = 8.64$ rad is presented. As is seen in Fig. 4, the peak–valley phase error does not exceed 0.15 rad (in the case presented in Fig. 4 this error is equal to 0.065 rad). The rms error is near 0.011 rad.

Figure 5 shows the experimental curve for the histogram of phase errors in Fig. 4 in the range of PV error, in percent. A PV error range of 100% means the maximum span of the PV phase error of phase estimation in Fig. 4. We used the Monte Carlo method and estimated errors by generation of the 1024 data series. By using Pirson criteria we found out that the probability density of this estimation is similar to that of Gaussian noise; this similarity confirms the correctness of nonlinear filtering procedure.

Let us consider the results of processing a signal with a more complex model [Eq. (7)] with variable envelope and nonuniform background.[28] An example of the signal realization is presented in Fig. 6(a). Note that in the signal model [Eq. (7)] nonuniform background is not taken into account, which leads to phase errors [Fig. 6(c)]. However, the value of the phase error is small, and the algorithm is not destabilized.

Since the influence of phase fluctuations on the signal value depends on the signal phase, it is similar to noise correlated with the signal. Phase filtering results presented in Figs. 3 and 6 show the noise immunity of the MNLF algorithm against correlated noise.

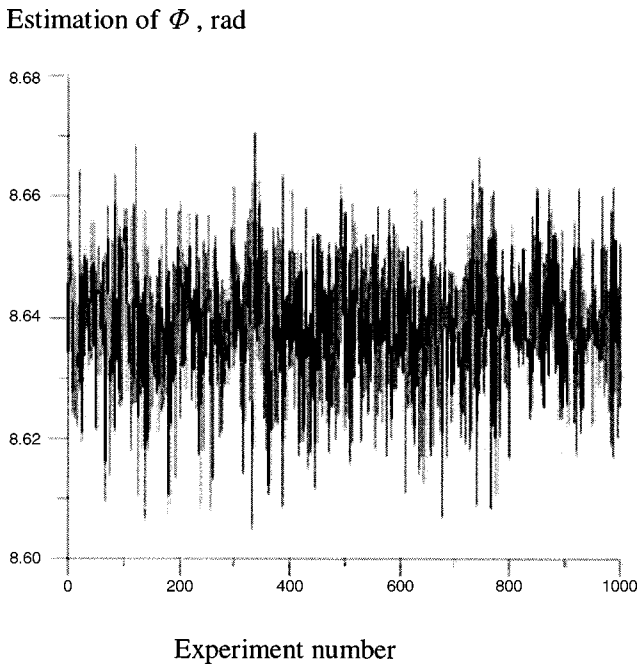

Fig. 4. Typical phase error of the MNLF algorithm.

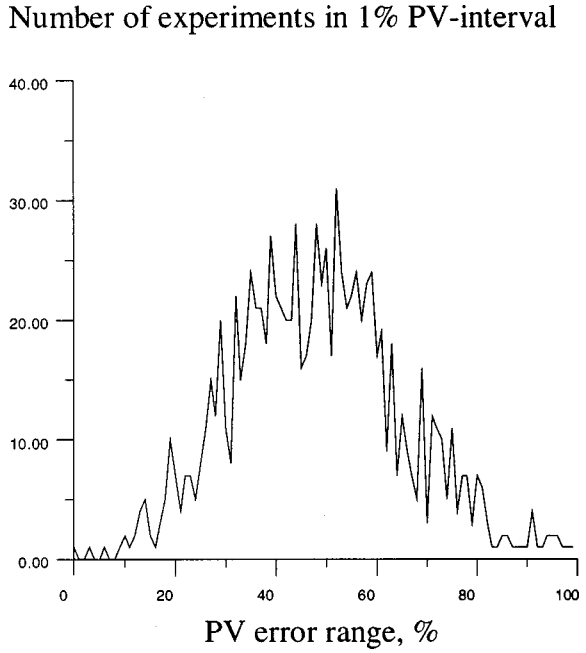

Fig. 5. Histogram of the phase error (the estimated phase error is presented in Fig. 4).

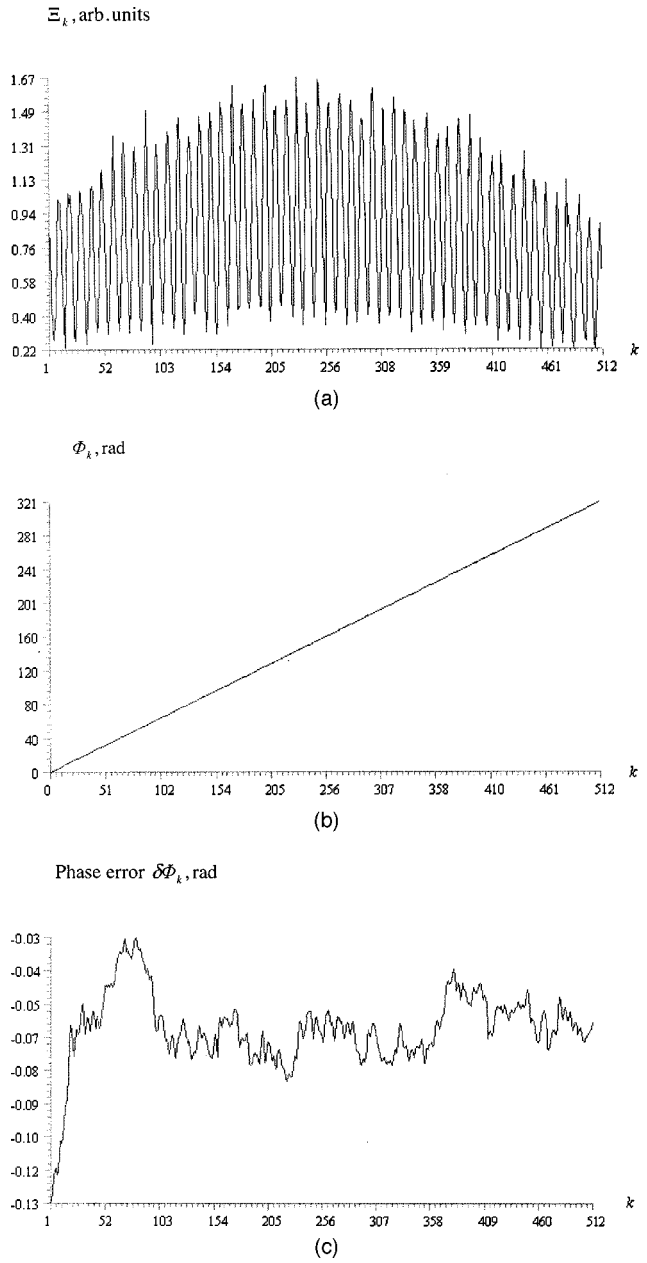

Fig. 6. Reconstruction of the phase function in the case of variable envelope and nonuniform background: (a) intensity distribution, (b) phase function, and (c) phase error.

4. CONCLUSIONS

The MNLF algorithm gives phase estimates [Eqs. (11)] by predicting the value of the vector of parameters for the next step by using all the information available from the current step. The last estimation is the most accurate. The necessary number of steps L can be taken to reduce rms error as $\sqrt{L}$.

The main advantages of the Markov nonlinear filtering method are the following. It gives the optimal estimates of signal parameters that depend nonlinearly on the signal meaning. The algorithm is optimized for minimizing phase errors under the influence of phase fluctuations and of noise correlated with the signal. Since the algorithm of Markov filtering is written not in integral form but in recurrent form, it reduces a number of calculations and the amount of memory required. It also increases the accuracy of the estimation of noisy data and allows one to work in a real-time scale of data receiving. The phase unwrapping problem is solved automatically, and the interval of the phase restoration is not restricted to 2π rad as in conventional PSI methods.

The considered version of the filtering algorithm was applied to the PSI method (multichannel data), but it also can be used for determination of single two-dimensional-interference-pattern phase characteristics (multidimensional observed data) in a wide range of change of intensity distribution parameters.[26,27] With this method, phase fluctuations and correlated additive noise influence is effectively decreased according to a strict optimum criterion, which is an essential advantage of the presented method in comparison with conventional estimation methods of interference-pattern phase characteristics.

The accuracy of the MNLF can be increased by iteration processing of the data series.

APPENDIX A

Let us assume that components of the vector $\mathbf{\Theta}$ are defined by Markov stochastic process properties. The probability density function $p(x, \mathbf{\Theta})$ of the Markov process $\mathbf{\Theta}$ complies with the Stratonovich stochastic equation,[23]

$$\frac{\partial p(x,\mathbf{\Theta})}{\partial t} = \mathbf{T}\{p(x,\mathbf{\Theta})\} + \frac{2}{N_0}p(x,\mathbf{\Theta}) \times \{\xi(x)s(x,\mathbf{\Theta}) - s(x,\mathbf{\Theta})\mathbf{M_{ps}} \times [s(x,\mathbf{\Theta})] - \xi(x)\mathbf{M_{ps}}[s(x,\mathbf{\Theta})] + (\mathbf{M_{ps}}[s(x,\mathbf{\Theta})])^2\}, \quad \text{(A1)}$$

where $\mathbf{M_{ps}}[\cdot] = \int_{-\infty}^{\infty}\cdots\int_{-\infty}^{\infty}(\cdot)p(x,\mathbf{\Theta})\Pi_{i=1}^{n}d\Theta_i$ is the *a posteriori* expected value and $\mathbf{T}\{.\}$ is a Fokker–Planck operator that has the form

$$\mathbf{T}\{p(x,\mathbf{\Theta})\} = -\frac{\partial}{\partial\mathbf{\Theta}}[\mathbf{F}(x,\mathbf{\Theta})p(x,\mathbf{\Theta})] + \frac{1}{2}\frac{\partial^2}{\partial\mathbf{\Theta}^2} \times [\mathbf{N}(x)p(x,\mathbf{\Theta})].$$

Generally the solution of Eq. (A1) is quite complex. An approximation of the probability density function and a decomposition of nonlinear functions[23] are usually used. The probability density function is approximated by functions that depend on a limited number of arguments. The frequent assumption is about the normality of the probability density function. The basis for this assumption is that when the signal-to-noise ratio and the observation time period are large enough, an *a posteriori* distribution approximates the normal distribution. This kind of approximation is called the Gaussian approximation.[23] Below we will consider the Gaussian approximation of the second order.

In the general case, when the multichannel interferometric signal $\mathbf{S}_m$ [Eq. (3)] is considered, these approximations give the discrete estimation of the vector $\mathbf{\Theta}$ at the point x_k:

$$\mathbf{\Theta}_k = \mathbf{\Theta}_k^{k-1} + \mathbf{R}_k^{k-1}\left\{\left(\frac{\partial}{\partial \mathbf{\Theta}_k^{k-1}}\right)^{\mathbf{T}}\right\}\mathbf{S}^{\mathbf{T}}(x_k, \mathbf{\Theta}_k^{k-1}) \times \mathbf{L}_k^{-1}\left[\mathbf{\Theta}_k - \mathbf{S}(x_k, \mathbf{\Theta}_k^{k-1}) - \frac{1}{2}\mathbf{B}_2\right], \tag{A2}$$

$$\mathbf{R}_k = \mathbf{R}_k^{k-1} - \mathbf{R}_k^{k-1}\left\{\left(\frac{\partial}{\partial \mathbf{\Theta}_k^{k-1}}\right)^{\mathbf{T}}\right\}\mathbf{S}^{\mathbf{T}}(x_k, \mathbf{\Theta}_k^{k-1}) \times \mathbf{L}_k^{-1}\left[\left\{\left(\frac{\partial}{\partial \mathbf{\Theta}_k^{k-1}}\right)^{\mathbf{T}}\right\}\mathbf{S}^{\mathbf{T}}(x_k, \mathbf{\Theta}_k^{k-1})\right]^{\mathbf{T}}\mathbf{R}_k^{k-1}, \tag{A3}$$

where $\mathbf{\Theta}_k^{k-1}$, $\mathbf{R}_k^{k-1}$ are the values of the vector of parameters and the covariance matrix, respectively, in step x_k, which is predicted from the step x_{k-1},

$$\mathbf{B}_2 = \left\{\left[\mathbf{R}_k^{k-1}\left(\frac{\partial}{\partial \mathbf{\Theta}_k^{k-1}}\right)^{\mathbf{T}}\right]^{\mathbf{T}}\left(\frac{\partial}{\partial \mathbf{\Theta}_k^{k-1}}\right)^{\mathbf{T}}\right\}\mathbf{S}(x_k, \mathbf{\Theta}_k^{k-1}), \tag{A4}$$

$$\mathbf{L}_k = \mathbf{N}_a + \left[\left\{\left(\frac{\partial}{\partial \mathbf{\Theta}_k^{k-1}}\right)^{\mathbf{T}}\right\}\mathbf{S}^{\mathbf{T}}(x_k, \mathbf{\Theta}_k^{k-1})\right]^{\mathbf{T}} \times \mathbf{R}_k^{k-1}\left\{\left(\frac{\partial}{\partial \mathbf{\Theta}_k^{k-1}}\right)^{\mathbf{T}}\right\}\mathbf{S}^{\mathbf{T}}(x_k, \mathbf{\Theta}_k^{k-1}) + \frac{1}{2}\mathbf{B}_3, \tag{A5}$$

$$[\mathbf{B}_3]_{ij} = \sum_{p,q,r,l=1}^{n} \frac{\partial^2 s_i(x_k, \mathbf{\Theta})}{\partial \Theta_p \partial \Theta_q} r_{pr} r_{ql} \frac{\partial^2 s_j(x_k, \mathbf{\Theta})}{\partial \Theta_r \partial \Theta_l}. \tag{A6}$$

Expressions in curly brackets in Eqs. (A2)–(A5) are the operators that should be applied to the next function, and $\mathbf{N}_a$ is the intensity matrix of the vector additive noise, $[\mathbf{N}_a]_{ij} = {\sigma_a}^2$, $i = j$, $[\mathbf{N}_a]_{ij} = 0$, $i \neq j$. Components of the vector $\mathbf{\Theta}$ and the covariance matrix $\mathbf{R}$ in Eq. (A6) are the values predicted from the previous step, and upper indices are omitted to simplify the notation.

The prediction of the vector of parameters and the covariance matrix in step x_k from step x_{k-1} is carried out by use of Eqs. (9) with various methods. For example, the simplest way to predict the vector of parameters is

$$\mathbf{\Theta}_k^{k-1} = \mathbf{F}(x, \mathbf{\Theta}_{k-1}),$$

where the argument step Δx is assumed to be equal to 1.

As mentioned above, Eqs. (A2)–(A3) define the algorithm for estimation of $\mathbf{\Theta}$ and $\mathbf{R}$ in the general case, when a vector of interferometric data is processed. In this paper a scalar signal is considered, and $\mathbf{S}^{\mathbf{T}}(x_k, \mathbf{\Theta}_k^{k-1}) = S(x_k, \mathbf{\Theta}_k^{k-1})$. With this the $\mathbf{B}_3$ matrix in Eq. (A6) consists of only one element, B_3. The vector of derivatives according to signal model Eqs. (4) and (7) has the following form:

$$\mathbf{D}_k = \left\{\left(\frac{\partial}{\partial \mathbf{\Theta}_k^{k-1}}\right)^{\mathbf{T}}\right\}S(x_k, \mathbf{\Theta}_k^{k-1}) = (-A\exp[-(C_k^{k-1})^2]V_k^{k-1}\sin[\Phi_k^{k-1} + (N_{ph})_k^{k-1}], 0, -AC_k^{k-1}\exp[-(C_k^{k-1})^2]\{1 + V_k^{k-1} \times \sin[\Phi_k^{k-1} + (N_{ph})_k^{k-1}]\}, 0, 0, -A\exp[-(C_k^{k-1})^2]V_k^{k-1}\sin[\Phi_k^{k-1} + (N_{ph})_k^{k-1}])^{\mathbf{T}}. \tag{A7}$$

In this equation, the U, B, V derivatives of the vector of parameters are considered to be equal to 0, since we assumed for simplicity that their meanings do not change with increasing k. For $\mathbf{B}_2$ in the case of a scalar signal we can use the equation

$$B_2 = \sum_{i,j=1}^{6} r_{ij}\frac{\partial^2 S(x_k, \mathbf{\Theta}_k^{k-1})}{\partial \Theta_i \partial \Theta_j}, \tag{A8}$$

where r_{ij} are the components of the covariance matrix and Θ_i are the components of the vector of parameters.

According to Eq. (A7) we can reduce this expression to the form

$$B_2 = \frac{\partial^2 S}{\partial \Phi^2}(r_{11} + 2r_{16} + r_{66}) + \frac{\partial^2 S}{\partial \Phi \partial C}(2r_{13} + 2r_{63}) + \frac{\partial^2 S}{\partial C^2}r_{33}. \tag{A9}$$

The term B_3 is reduced in the same way as Eq. (A8). Taking into account all the simplifications described above, the estimation algorithm in Eqs. (A2)–(A3) is transformed into the Eq. (11) algorithm.

For a simple case of constant envelope and background components that we use for computer simulations, coefficients B_2 and B_3 have the following form:

$$B_2 = \frac{\partial^2 S}{\partial \Phi \partial \Phi}(r_{11} + 2r_{14} + r_{44}),$$

$$B_3 = \left(\frac{\partial^2 S}{\partial \Phi \partial \Phi}\right)^2(r_{11} + 2r_{14} + r_{44})^2.$$

REFERENCES

1. J. H. Bruning, D. R. Herriott, J. E. Gallagher, D. P. Rosenfeld, A. D. White, and D. J. Brangaccio, "Digital wave-front measuring interferometer for testing optical surfaces and lenses," Appl. Opt. **13**, 2693–2703 (1974).
2. J. C. Wyant, "Interferometric optical metrology: basic principles and new systems," Laser Focus **18**, 65–71 (1982).
3. K. Creath, "Phase measurement interferometry technique," Prog. Opt. **26**, 349–383 (1988).
4. M. Takeda, H. Ina, and S. Kobayashi, "Fourier-transform method of fringe-pattern analysis for computer-based topography and interferometry," J. Opt. Soc. Am. **72**, 156–160 (1982).
5. D. W. Robinson, "Automatic fringe analysis with a computer image-processing system," Appl. Opt. **22**, 2169–2176 (1983).
6. C. Roddier and F. Roddier, "Interferogram analysis using Fourier transform techniques," Appl. Opt. **26**, 1668–1683 (1987).
7. R. Jozwicki, M. Kujawinska, and L. Salbut, "New contra old

wavefront measurement concepts for interferometric optical testing," Opt. Eng. **31**, 422–433 (1992).
8. S. M. Pandit, N. Jordache, and G. A. Joshi, "Data-dependent system methodology for noise-insensitive phase unwrapping in laser interferometric surface characterization," J. Opt. Soc. Am. A **11**, 2584–2592 (1994).
9. I. P. Gurov and I. M. Nagibina, "The structure of multichannel interference measuring systems for precision control of the objects geometric characterization," Izv. Vyssh. Uchebn. Zaved. Priborostr. **34**, 59–66 (1991) (in Russian).
10. A. Papoulis, *Systems and Transforms with Applications in Optics* (McGraw-Hill, New York, 1968).
11. H. J. Nussbaumer, *Fast Fourier Transform and Convolution Algorithms* (Springer-Verlag, Berlin, 1982).
12. J. E. Grevenkamp and J. H. Bruning, "Phase-shifting interferometry," in *Optical Shop Testing*, D. Malacara, ed. (Wiley, New York, 1992).
13. D. K. Bowen, D. G. Chetwynd, and D. R. Schwarzenberger, "Sub-nanometre displacements calibration using x-ray interferometry," Meas. Sci. Technol. **1**, 107–119 (1990).
14. P. Hariharan, B. F. Oreb, and T. Eiju, "Digital phase-shifting interferometry: a simple error-compensating phase calculation algorithm," Appl. Opt. **26**, 2504–2506 (1987).
15. G. Lai and T. Yatagai, "Generalized phase-shifting interferometry," J. Opt. Soc. Am. A **8**, 822–827 (1991).
16. C. T. Farrell and M. A. Player, "Phase step measurement and variable step algorithms in phase shifting interferometry," Meas. Sci. Technol. **3**, 953–958 (1992).
17. Y. Sarrel, "Phase stepping: a new self-calibrating algorithm," Appl. Opt. **32**, 3598–3600 (1993).
18. G. S. Han and S. W. Kim, "Numerical correction of reference phases in phase-shifting interferometry by iterative least-squares fitting," Appl. Opt. **33**, 7321–7325 (1994).
19. K. Hibino, B. F. Oreb, D. I. Farrant, and K. G. Larkin, "Phase shifting for nonsinusoidal waveform with phase-shift errors," J. Opt. Soc. Am. A **12**, 761–767 (1995).
20. E. Lloyd, ed. *Statistics*, Vol. 6 of Handbook of Applicable Mathematics, Walter Ledermann, ed. (Wiley, Chichester, UK, 1984).
21. P. J. de Groot, "Vibration in phase-shifting interferometry," J. Opt. Soc. Am. A **12**, 354–365 (1995).
22. J. Schwider, R. Burow, K. E. Ellsner, J. Grzanna, R. Spolaczyk, and K. Merkel, "Digital wave-front measuring interferometry: some systematic error sources," Appl. Opt. **22**, 3421–3432 (1983).
23. M. S. Yarlykov and M. A. Mironov, *Markov Theory of Stochastic Processes Estimation* (Radio I svyaz, Moscow, 1993) (in Russian).
24. R. E. Kalman and R. S. Bucy, "New results in linear filtering and prediction theory," Basic Eng. **82**, 35–40 (1960).
25. V. I. Tikhonov and M. A. Mironov, *Markov Processes* (Soviet Radio, Moscow, 1977) (in Russian).
26. I. P. Gurov and D. V. Sheynikhovich, "Noise-immune phase-shifting interferometric system based on Markov non-linear filtering method," in *Statistical and Stochastic Methods for Image Processing*, E. R. Dougherty, F. Preteux, and J. L. Davidson, eds., Proc. SPIE **2823**, 121–125 (1996).
27. I. P. Gurov and D. V. Sheynihovich, "Non-linear phase estimation by computer-aided Markov filtering method: accuracy investigations," in *Proceedings of the IEEE TENCON '96 Conference, Perth, Australia* (Institute of Electrical and Electronics Engineers, New York, 1996), Vol. 2, pp. 758–762.
28. I. P. Gurov and D. V. Sheynikhovich, "Determination of phase characteristics of an interference pattern by the method of nonlinear Markov filtering," Opt. Spectrosc. (USSR) **83**, 137–142 (1997).